Original Article

Contribution of serotonin to cardiac remodeling associated with hypertensive diastolic ventricular dysfunction in rats

Estelle Ayme-Dietrich[a,*], Halim Marzak[a,*], Roland Lawson[a], Walid Mokni[a], Olivia Wendling[b], Roy Combe[b], Julien Becker[b], Lahcen El Fertak[b], Marie-France Champy[b], Rachel Matz[c], Ramaroson Andriantsitohaina[d], Stéphane Doly[e], Katia Boutourlinsky[e], Luc Maroteaux[e], and Laurent Monassier[a,b]

Objective: Left-ventricular hypertrophy and interstitial fibrosis are the main pathophysiological factors of heart failure with preserved ejection fraction. Blockade of the serotonin 5-HT_{2B} receptor (5-HT_{2B}R) has been shown to reduce cardiac hypertrophy, oxidative stress, and extracellular cell matrix activation. In this study, we evaluated the effects of the 5-HT_{2B}R blockade, on hemodynamic and cardiac remodeling, in spontaneously hypertensive rats (SHRs) that display a diastolic dysfunction with preserved ejection fraction.

Method: Thirty-seven-week-old SHRs were randomized in four groups receiving either saline, the selective 5-HT_{2B}R antagonist RS-127445 (1 mg/kg per day), a calcium channel blocker nicardipine (6 mg/kg per day), or RS-127445 + nicardipine. During the 14 weeks of treatment period, cardiac function and blood pressure were monitored by echocardiography and tail-cuff. Finally, electrocardiograms and invasive hemodynamics were obtained before blood collection. Heart was analyzed for morphology and mRNA expression. A complementary study evaluated the cardiac and vascular effects of serotonin on wild-type and mice knockout for the 5-HT_{2B}R ($Htr_{2B}^{-/-}$) and/or the 5-HT_{2A}R ($Htr_{2A}^{-/-}$).

Results: Despite the left ventricular 5-HT_{2B}R overexpression, 5-HT_{2B}R blockade by RS-127445 did not affect left ventricular hypertrophy and fibrosis in SHRs. This antagonist did not improve diastolic dysfunction, neither alone nor in combination with nicardipine, although it induced plasma brain natriuretic peptide decrease. Moreover, RS-127445 amplified subendocardial fibrosis and favored left ventricular dilatation. Finally, a subendocardial left ventricular fibrosis was induced by chronic serotonin in wild-type mice, which was increased in $Htr_{2B}^{-/-}$ animals, but prevented in $Htr_{2A}^{-/-}$ and $Htr_{2A/2B}^{-/-}$ mice, and could be explained by a contribution of the endothelial 5-HT_{2B}Rs to coronary vasodilatation.

Conclusion: This work is the first to identify a cardioprotective function of the 5-HT_{2B}R in an integrated model of diastolic dysfunction with preserved ejection fraction.

Keywords: 5-HT_{2B} receptors, fibrosis, hypertension, hypertrophy, serotonin, spontaneously hypertensive rats

Abbreviations: BNP, brain natriuretic peptide; BP, blood pressure; DAP, diastolic arterial pressure; DD-PEF, diastolic dysfunction with preserved ejection fraction; EDLVD, left-ventricular end-diastolic diameter; ESLVD, left-ventricular end-systolic diameter; HF-PEF, heart failure with preserved ejection fraction; HR, heart rate; IVRT, isovolumetric relaxation time; LV, left ventricle; LVM, left ventricular mass; LVSP, left-ventricular systolic pressure; SAP, systolic arterial pressure; SHRs, spontaneously hypertensive rats; WKYs, Wistar–Kyoto rats

INTRODUCTION

About half of the patients with heart failure exhibit a left-ventricular ejection fraction over 40–50% [1,2] [heart failure with preserved ejection fraction (HF-PEF)]. Observed in the elderly, patients are mainly women with a long history of high blood pressure and obesity. Current treatments do not improve the survival of patients with HF-PEF [3,4], and the mortality remains high with a comparable prognosis to patients with an altered ejection fraction. This therapeutic failure is, at least in part, due to the missing knowledge about pathophysiological

Journal of Hypertension 2015, 33:2310–2321

[a]Laboratoire de Neurobiologie et Pharmacologie Cardiovasculaire EA7296, Faculté de Médecine, Fédération de Médecine Translationnelle, Université et Centre Hospitalier de Strasbourg, Strasbourg, [b]Mouse Clinical Institute, Illkirch-Graffenstaden, [c]CNRS, UMR7213, University of Strasbourg, Illkirch-Graffenstaden, [d]INSERM U1063, Stress oxydant et pathologies métaboliques, LUNAM Université, Angers and [e]INSERM UMR S-839, Institut du Fer à Moulin, Université Pierre et Marie Curie, 17 rue du Fer à Moulin, Paris, France

Correspondence to Laurent Monassier, MD, PhD, Laboratoire de Neurobiologie et Pharmacologie Cardiovasculaire, Faculté de Médecine, 11 rue Humann, 67085 Strasbourg, Cedex, France. Tel: +33 368853392; fax: +33 368853388; e-mail: laurent.monassier@unistra.fr

*Estelle Ayme-Dietrich and Halim Marzak contributed equally to this work.

Received 13 April 2015 **Revised** 9 June 2015 **Accepted** 9 June 2015

DOI:10.1097/HJH.0000000000000695

mechanisms underlying the disease. Identified pathological features include cardiomyocytes hypertrophy, cardiac fibrosis, ischemia with endothelial dysfunction, and local inflammation that contribute to diastolic dysfunction and arterial stiffening.

Recent studies have emphasized the role of G-protein-coupled receptors (GPCRs) in the initiation of processes that play crucial roles in myocytes hypertrophy, cardiac release of various cytokines, and fibroblast stimulation [5,6]. Serotonin [5-hydroxytryptamine (5-HT)] effects are mediated by actions on numerous cognate receptors belonging to the GPCRs and ionotropic families. Activation of the 5-HT$_2$G$_q$/G$_{11}$-coupled subtypes participates in cell growth and proliferation. We have previously shown that the 5-HT$_{2B}$ receptor (5-HT$_{2B}$R) regulates cardiomyocyte growth during cardiac embryonic development, and that its pharmacologic or genetic blockade can prevent left ventricular hypertrophy triggered by β-adrenergic and angiotensin II receptors type 1 [7,8]. Moreover, this blockade is associated with a reduction of the production of interleukin (IL)-1β, tumor necrosis factor (TNF)α, IL-6, and transforming growth factor (TGF)-β1, as well as oxidative stress via inhibition of the NAD(P)H oxidase [9,10]. We reported that these inhibitions originate from a regulation of non-cardiomyocyte cells and are without any significant hemodynamic side effect [9]. Independently, 5-HT$_{2B}$R blockade was shown to reduce cardiac hypertrophy in an aortic banding model of cardiac hypertrophy in rats [11]. Therefore, we hypothesized that 5-HT via the G$_q$-coupled 5-HT$_{2B}$R could participate in the pathophysiological mechanisms of diastolic dysfunction with preserved ejection fraction (DD-PEF). Recently, we have shown that spontaneously hypertensive rats (SHRs) progressively develop a DD-PEF that is very similar to hypertensive humans [12].

The first goal of this study was to investigate if the blockade of 5-HT$_{2B}$Rs by the highly selective antagonist RS-127445 [13] could slow the rate of cardiac function alterations and remodeling in SHRs during the natural course of hypertension. Taking into account that, in previous studies, the blockade of these receptors did not affect blood pressure; we compared 5-HT$_{2B}$R antagonist effects to the calcium channel blocker, nicardipine, and analyzed the effects of a combination of both. Having observed that RS-127445 treatment amplified ventricular dilation and fibrosis, a second part of the study was designed to confirm these results in investigating the contribution of 5-HT-induced myocardial fibrosis in mice lacking 5-HT$_{2A}$Rs (*Htr*$_{2A}^{-/-}$), 5-HT$_{2B}$Rs (*Htr*$_{2B}^{-/-}$), and both (*Htr*$_{2A/2B}^{-/-}$). Finally, we studied coronary blood flow from isolated hearts *Htr*$_{2B}^{-/-}$ mice, and the effects of a 5-HT$_2$R selective agonist in isolated aorta. This last part identified the contribution of the endothelial 5-HT$_{2B}$R to arterial vasodilatation.

METHODS

Animals and experimental procedures

Twenty-week-old SHRs and their normotensive Wistar–Kyoto (WKY) counterparts were obtained from Janvier, France. Rats were group-housed 2–3 per cage. They were maintained under standard conditions in the animal facilities, with an ambient temperature of 22 ± 1°C and a 12-h light–dark cycle (lights on 06 : 00–18 : 00 hours). Food and water were available *ad libitum*. At the age of 36 weeks, blood pressure and heart rate (HR) were measured by the tail-cuff technique before the evaluation of cardiac anatomy and function by echocardiography. The 37-week-old SHRs were then randomized into four treatment groups that were treated for 14 weeks until the animals were 51 weeks of age: hypertensive controls (SHR-C), SHRs treated with the selective 5-HT$_{2B}$ receptor antagonist RS-127445 (Tocris, Bristol, UK) (SHR-RS), SHRs treated with the calcium blocker nicardipine (Aguettant, Lyon, France) (SHR-N), and SHRs treated by the combination of nicardipine and RS-127445 (SHR-NRS). Cardiac function and anatomy were regularly analyzed by echocardiography in 43 and 51-week-old animals, and blood pressure was measured by the tail-cuff method at the age of 51 weeks. RS-127445 (1 mg/kg per 24 h) was administered in two intraperitoneal injections at 0800 and 1800 h. Nicardipine (6 mg/kg per day) was administered intraperitoneally in one single daily injection at 1800 h. All animals received three injections every day with an active compound or its vehicle depending on the group. All along the treatment period, animals were weighted every week. Water and food consumptions were evaluated every 3 days. At the end of the study, all animals were anesthetized with sodium pentobarbital for ECG recordings and left ventricular catheterization. Before euthanasia by a pentobarbital overdose, blood was collected via a jugular venous catheter. Plasma was obtained by centrifugation (10000 r.p.m. for 10 min, at 4°C) and stored at −80°C until use. The heart was immediately excised and weighed. The apex was flash-frozen in liquid nitrogen and stored at −80°C until use. The remaining heart was fixed in 4% paraformaldehyde phosphate-buffered saline (PBS) solution.

Ten-week-old male 129S2/SvPAS (*Htr*$_{2B}^{+/+}$, provided from Charles River France), *Htr*$_{2A}^{-/-}$ [14], *Htr*$_{2B}^{-/-}$ [15], and *Htr*$_{2A/2B}^{-/-}$ mice on the same genetic background were given daily intraperitoneal 5-HT injections for 5 consecutive days (one initial injection at 50 mg/kg, followed by a daily injection at 20 mg/kg during 4 days); controls were given five saline injections. 5-HT was dissolved in saline just before injection. After euthanasia, hearts were frozen and sectioned in a cryostat in the frontal plane, through the aortic arch, and down to the apex. Immunohistochemical staining for proliferating cells was performed with the monoclonal antibody Ki-67. Masson's trichrome and immunostaining using anti-vimentin antiserum were used to visualize, respectively, collagen and fibroblasts. For Ki-67, 10 fields (magnification 20×) were counted per heart (15 sections per mice, 8 mice per group); the mean number of Ki-67-positive cells per field is given on the graph (see Fig. 5 below). For vimentin quantification, fluorescence intensity was measured in fibrotic areas (magnification 20×) using image J software, independently of any surface quantification. All antibodies were from Santa Cruz (Santa Cruz Biotechnology, Santa Cruz, California, USA). No quantification was performed on Masson's trichrome staining.

The animal facilities were legally registered for animal housing and experimentation, and the scientists in charge of the experiments were in possession of the certificate

authorizing experimentation on living animals, delivered by the governmental veterinary office. All procedures were performed in accordance with the guidelines for animal experimentation of the European Communities Council Directive EU/63/2010.

Blood pressure measurements

Systolic arterial pressure (SAP) and HR were taken in the morning (0800 h) by means of a noninvasive automatic blood pressure device (Letica LE2002, Spain) after a previous 5-min long heat-induced tail artery vasodilatation, in a small heating room (36–37°C) (Letica LE5610, Spain), the rat being placed in an adapted restrainer. The mean value of the five readings from each animal was considered.

Echocardiography and Doppler

Transthoracic echocardiography was performed in rats anesthetized with 1.5–2% isoflurane using a Sonos 5500 (Philips, USA) equipped with a 12-MHz sectorial transducer. Short and long-axis views and four and five-chamber apical cardiac views were used for measurements with a sonographer blinded to the experimental groups. Left-ventricular end-diastolic (EDLVD) and end-systolic (ESLVD) diameters, diastolic posterior wall and septal wall thicknesses were obtained from M-mode tracings of the left ventricle (LV) in the long-axis view. Left-atrial surface was measured from the four chambers apical view excluding the left auricle. Left ventricular mass (LVM) was calculated as $\mathrm{LVM} = 1.04 \times [(\mathrm{EDLVD} + \mathrm{PW} + \mathrm{SW})^3 - \mathrm{EDLVD}^3]$. The left ventricular systolic function was analyzed by axial and longitudinal components. Shortening fraction was calculated as $\mathrm{SF} = [(\mathrm{EDLVD} - \mathrm{ESLVD})/\mathrm{EDLVD}]$. Systolic lateral mitral annulus movement (lateral S_a) and systolic posterior wall movement (septal S_a) were obtained from the apical view using pulsed Doppler tissue imaging at a frame speed of 150 mm/s. The evaluation of left ventricular diastolic function was performed with indexes measured from the four-chamber apical view. Mitral inflow was recorded by placing the pulsed Doppler window at the tip of the mitral valve. We measured maximal velocities of the E and A waves to obtain the E/A ratio and the deceleration time of the E wave. The isovolumetric relaxation time (IVRT) was measured as the interval between aortic closure and the start of the mitral flow. Early mitral flow propagation velocity (V_p) was measured using color M-mode Doppler of the mitral flow. Early motion of the mitral annulus was obtained at its septal and lateral corners by pulsed Doppler tissue imaging. Left ventricular filling indexes (E/E lat and E/E septal) were calculated. All measured and calculated indexes are presented as the average of three consecutive beats.

ECG and invasive hemodynamic

All measurements were obtained in sodium pentobarbital-anesthetized rats (50 mg/kg, intraperitoneally). After induction of the anesthesia, rats were placed in dorsal position and recorded with the four arms of the ECG leads attached at the origin of each paw by unipolar and bipolar lead derivations with an electrocardiograph (CardioMax FX-3010, Fukuda Denshi, Japan). Maximal amplitude of the R wave and electrical sign of cardiac hypertrophy were measured manually.

Then animals were tracheotomized and left on spontaneous breathing. A saline-filled polyethylene catheter was introduced into the left ventricle through the right carotid artery and connected to a Statham Db23 transducer that was in turn connected to a data acquisition and storage system (IOX, EMKA Technologies, France). From left ventricular tracings, left ventricular systolic pressure (LVSP) and left ventricular end-diastolic pressure (LVEDP) were measured. The first derivative of the left ventricular pressure was calculated. Its maximal (dP/dt_{max}) and minimal (dP/dt_{min}) values were, respectively, used to assess contractility and relaxation.

Histological examination

The basal part of the heart, 2 mm far from the mitral annulus, was fixed, paraffin-embedded, and sectioned (5 μm) using standard techniques. Interstitial and perivascular myocardial collagen contents were analyzed on picro-Sirius red-stained paraffin sections.

Cardiac images were captured with the aid of a light camera-equipped microscope, with a 10-fold magnification for coronary arteries and 5-fold magnification for larger myocardial areas. For each rat's cardiac slice, two images of different focal fibrosis areas and two images outside these areas were recorded for interstitial fibrosis measurements. Four coronary arteries pictures were taken for perivascular fibrosis assessment. Interstitial fibrosis detection was performed using a color threshold method with Image J software, marking the red-stained collagen fibers and then converting it into a pixel number. Interstitial fibrosis was then normalized by the total surface (in pixels) of the analyzed region and expressed in percentage. The epicardium, coronary vessels, and papillary muscles were removed from the images before quantification. Perivascular fibrosis was measured by surface assessment of the regions of interest with Image J software. Perivascular fibrosis was expressed as the ratio of the surface of the adventitia layer to the surface of the vessel (lumina + media + adventitia). Large and medium coronary arteries (diameter of lumina + media > 130 μm; mean 170 ± 24 μm) and small coronary arteries (diameter of lumina + media < 130 μm; mean 85 ± 18 μm) were considered separately.

For immunohistochemistry of 5-HT_{2A}R in rats, the histological sections from paraffin-embedded tissues were collected on glass slides, treated with 10 mmol/l sodium citrate buffer (pH 6.0) in a bath at 94°C for 40 min. Then, the sections were incubated overnight at 4°C with the rabbit polyclonal antibody 5-HT_{2A}R (1/200, MBS175200, MyBiosource, USA) and the signal was amplified using the elite vectastain ABC technique (PK-6101, Vector), according to the manufacturer's instructions. Peroxidase was revealed using AEC kit (Vector).

Gene expression by RT-quantitative polymerase chain reaction

Total mRNA was extracted from rat cardiac apex using RNeasy Mini Kit QIAGEN. The concentration of total RNA was determined by UV spectrophotometry at 260/280 nm. The complementary DNAs were obtained by reverse transcription using Kit iScript complementary

TABLE 1. Primer sequences

Gene	Primer	Sequences (5′-3′)
GAPDH	Forward	GCAAGAGAGAGGCCCTCAG
	Reverse	TGTGAGGGAGATGCTCAGTG
5-HT_{2A}R	Forward	TTCACCACAGCCGCTTCAA
	Reverse	ATCCTGTAGTCCAAAGACTGGGATT
5-HT_{2B}R	Forward	GGCTGATTTGCTGGTTGGATTG
	Reverse	GGGCCATGTAGCCTCAAACATG
SERT 1	Forward	CATCAGCCCTCTGTTTCTCC
	Reverse	TAGCCCAAGACGATACTCCA

5-HT_{2A}R, 5-hydroxytryptamine $_{2A}$ receptor; 5-HT_{2B}R, 5-hydroxytryptamine $_{2B}$ receptor; GAPDH, glyceraldehyde 3-phosphate dehydrogenase; SERT, serotonin transporter.

deoxyribonucleic acid Synthesis BioRad. Semi-quantitative reverse transcription–PCR (RT-PCR) was produced on an amplification system (PCR LightCyclerCaroussel) with the kit LightCycler FastStart DNA Master Plus SYBR Green I from Roche (France). Table 1 shows forward and reverse primer sequences for all analyzed genes. For each gene, the expression data were normalized to an endogenous control glyceraldehyde-3-phosphate dehydrogenase (GAPDH). The reactions were considered in duplicate and the mRNA levels of each gene were calculated according to the formula $2^{-\Delta CT}$, where ΔCT is the difference in threshold cycle (Ct) values between the target and the endogenous control.

Western blotting

The 51-week-old WKY rats ($n=6$) and SHRs ($n=5$) were used for the experiments. Heart was collected immediately after euthanasia, rinsed in PBS on ice, and the apex was flash-frozen in liquid nitrogen and stored at −80°C until use. Heart tissue (0.5 g/ml) was homogenized on ice in cold buffer (50 mmol/l Tris-HCl, pH 7.5, 50 mmol/l NaCl, 2% triton) containing protease and phosphatase inhibitors cocktail (Roche), and centrifuged (10 000*g*, 10 min, 4°C). The supernatant was collected and protein concentration measured (BCA protein assay). Proteins [10 (R-5HT_{2B}) or 20 (R-5HT_{2A}) μg] were loaded on a 10% polyacrylamide gel (TGX Stain-FreeFastCast Acrylamide Kit 10%; Biorad, France) and transferred to polyvinylidene fluoride membrane with TransBlot Turbo transfer system (Biorad). The membrane was blocked with 10% milk solution in Tris-buffered saline–Tween 20 (0.1%) during 1 h at room temperature. 5-HT_{2A}R and 5-HT_{2B}R were detected using, respectively, a rabbit polyclonal anti-R-5-HT_{2A} (MBS175200, MyBioSource, USA) and a mouse monoclonal anti-R-5-HT_{2B} (A72–1, BD Biosciences, France) antibodies (1 : 1000, overnight, 4°C). After incubation with appropriate horseradish peroxidase (HRP)-linked secondary antibody (Sigma-Aldrich, France), proteins were detected and quantified using the BioRad Chemidoc System. Total proteins normalization using Stain-Free Gels (Biorad) was used to normalize the 5-HTRs detection (Western Blot Normalization using Image Lab software, Biorad).

Brain natriuretic peptide plasma assay

Brain natriuretic peptide (BNP) plasma concentration was determined using a standard rat BNP kit (Millipore, USA).

Urinary and plasma hormones

Fourteen-week-old WKY rats ($n=8$) and SHRs ($n=8$) were placed during 48 h in individual metabolic cages. The 24-h urine was collected the second day on dark-covered vials containing 250 μl HCl 1N to prevent spontaneous catecholamines and monoamines oxidation. Epinephrine, norepinephrine, dopamine, and the 5-HT metabolite, 5-hydroxyindoleacetic acid (5-HIAA), were measured by means of HPLC with electrochemical detection. Results were normalized on the urinary volume of the past 24 h.

Isolated perfused heart preparation

Hearts from male mice (12–19 weeks, 23–25 g) anesthetized with sodium pentobarbital (60 mg/kg, intraperitoneally) and heparinized (500 U/kg, intraperitoneally) were excised and cannulated under iced Krebs–Henseleit buffer (at 4°C). They were then immediately perfused according to Langendorff, at 37°C and pH 7.4, with modified Krebs–Henseleit solution containing (mmol/l) NaCl 118, $NaHCO_3$ 24, KCl 4.7, KH_2PO_4 1.2, $MgSO_4$ 1.2, $CaCl_2$ 2.5, di-sodium EDTA 0.5, and glucose 10, gassed with 95%O_2/5%CO_2. Perfusion pressure was constant and equivalent to 100 cmH_2O. The coronary flow was recorded by collecting the effluent over a period of 60 s. Coronary flow was measured during all experiments. Coronary resistance was calculated as perfusion pressure/coronary flow. After 30 min stabilization, isolated hearts were submitted to cumulative addition of isoproterenol (from 10^{-10} to 10^{-7} mol/l) in the perfusion solution.

Vascular reactivity

Segments of 2 mm thoracic aorta cleaned of fat and connective tissue were mounted on a multiwire myograph system filled with physiological salt solution (PSS) under normalized tension as previously described [16]. The presence of a functional endothelium was confirmed by the ability of acetylcholine (1 μmol/l) to induce more than 50% relaxation of vessels precontracted with phenylephrine (1 μmol/l). Concentration–response curves were constructed by cumulative addition of α-methyl-5-hydroxytryptamine (AMS, 10 nmol/l to 30 μmol/l). Results are expressed in mN/mm aortic ring length.

Aortic cyclic guanosine monophosphate content

Thoracic and abdominal aorta were carefully cleaned of fat and connective tissue, and incubated at 37°C in the absence or presence of S-nitroso-N-acetyl-DL-penicillamine (SNAP) – a Nitric oxide donor – for 20 min in PSS containing 3-isobutyl-1-methylxanthine (IBMX to inhibit cyclic guanosine monophosphate (cGMP) degradation via cyclic nucleotide phosphodiesterases, 100 μmol/l) and gassed with 95% O_2–5% CO_2. The reaction was stopped by transferring the aorta into ice-cold HCl (0.1N). After homogenization of the tissue, the cyclic GMP content was determined by radioimmunoassay as previously described [17]. cGMP was expressed as pmol/μg DNA.

Data analysis and statistics

All values were expressed as mean ± SD. Statistical comparisons between two or more groups were performed

when appropriate using Student's unpaired *t* tests or repeated-measures analysis of variance (ANOVA), followed by post-hoc analysis with Bonferroni's test (GraphPad Software version 6.0; GraphPad Software, San Diego, California, USA). *P* less than 0.05 was considered statistically significant.

RESULTS

Spontaneously hypertensive rats as a model of diastolic dysfunction with preserved systolic function induced by chronic high blood pressure

As shown in our previous study [12] and in Supplementary data (Table 1, http://links.lww.com/HJH/A525), 36-week-old SHRs demonstrate a severe hypertension, tachycardia, and a concentric left ventricular hypertrophy. A progressive increase of the left atrium surface is simultaneously observed attesting an augmentation of the left atrium pressure. Compared to WKY rats, left ventricular systolic function is apparently normal in SHRs, as shown by the left ventricular shortening fraction and the systolic mitral annulus movement (S_a), measured by Doppler tissue imaging. Conversely, SHRs have a left ventricular early diastolic dysfunction. The IVRT is increased by 26% attesting a primary trouble of the left ventricular relaxation that could be partly masked by the increase in left atrium pressure as attested by a 15% increase of the E wave and a 16% decrease of the early mitral flow propagation velocity (V_p). Doppler tissue imaging at the mitral annulus confirms a problem of the longitudinal fibers' early relaxation as attested by the decrease in the early diastolic velocities of the mitral annulus both at lateral (E_m) (−29%) and septal corners (E_{pw}) (−35%). All these alterations get worse over time and were associated with interstitial myocardial fibrosis that was markedly increased in 51-week-old SHR-C as compared with WKY rats. Adventitial collagen content of large coronary arteries was not modified in SHR-C, but was significantly increased when considering small arteries [12].

Cardiac expression of the 5-HT$_{2A}$R, 5-HT$_{2B}$R, and the serotonin transporter

5-HT$_{2A}$R, 5-HT$_{2B}$R, and serotonin transporter (SERT) are expressed in the rat myocardium of both 51-week-old WKY rats and SHRs. In the LV of SHR-C, a three-fold overexpression of the 5-HT$_{2B}$R mRNA was observed and mRNA encoding for the 5-HT$_{2A}$R was increased by 25 times compared to WKY rats. A non-significant decrease of SERT mRNA expression was noticed in hypertensive animals (Fig. 1). At the protein level, we observed a 60% 5-HT$_{2B}$R overexpression (1.59 ± 0.19 vs. 1 ± 0.23; $P < 0.05$) and a three-fold increase in 5-HT$_{2A}$R (3.2 ± 0.29 vs. 1 ± 0.11; $P < 0.01$) in SHRs compared to WKY rats (Fig. 2a). The 5-HT$_{2A}$R expression was mainly found in coronary smooth muscle cells (Fig. 2b).

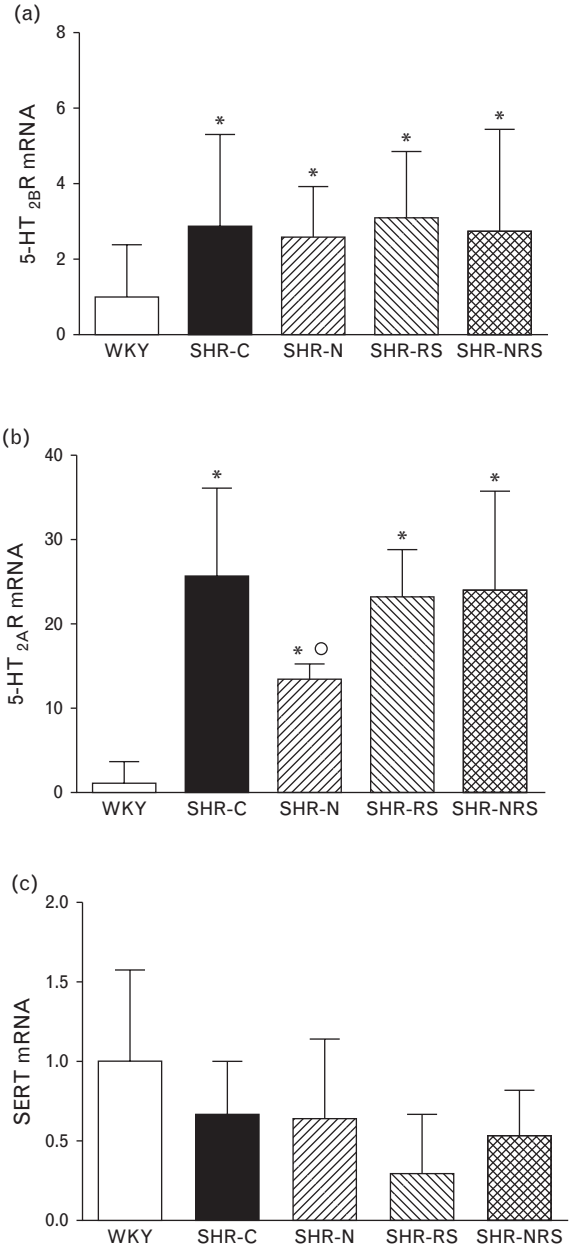

FIGURE 1 Left-ventricular expression of 5-HT$_{2B}$R (a), 5-HT$_{2A}$R (b), and (c) SERT mRNAs. Quantification was performed by real-time quantitative PCR from WKY rats, SHRs untreated (SHR-C), SHRs treated with nicardipine (SHR-N), SHRs treated with RS-127445 (SHR-RS), and SHRs treated with nicardipine and RS-127445 (SHR-NRS). The results are normalized to GAPDH and presented relative to WKY rats. Data are expressed as mean $2^{-\Delta\Delta Ct} \pm$ SEM. (*) $P < 0.05$ vs. WKY rats; (°) $P < 0.05$ vs. SHR-C ($n = 10$). 5-HT$_{2A}$R, 5-hydroxytryptamine $_{2A}$ receptor; 5-HT$_{2B}$R, 5-hydroxytryptamine $_{2B}$ receptor; SHRs, spontaneously hypertensive rats; WKY, Wistar–Kyoto rats.

Activities of the sympathetic and serotonergic systems in spontaneously hypertensive rats

To evaluate the activities of the sympathetic and serotonergic systems, we measured 24-h urinary epinephrine, norepinephrine, dopamine, and 5-HIAA. In SHRs, we observed an increase in urinary epinephrine (155 ± 25 vs. 69 ± 12 ng/24 h in WKYs; $P < 0.05$) and dopamine (4.4 ± 0.5 vs. 2.7 ± 0.3 μg/24 h in WKY rats; $P < 0.05$). Conversely, the 24-h urinary norepinephrine (1.14 ± 0.15 μg/24 h in SHRs vs. 1.27 ± 0.11 μg/24 h in WKY rats; $P > 0.05$) and 5-HIAA (34 ± 4 μg/24 h in SHRs vs. 37 ± 4 μg/24 h in WKY rats; $P > 0.05$) were not modified.

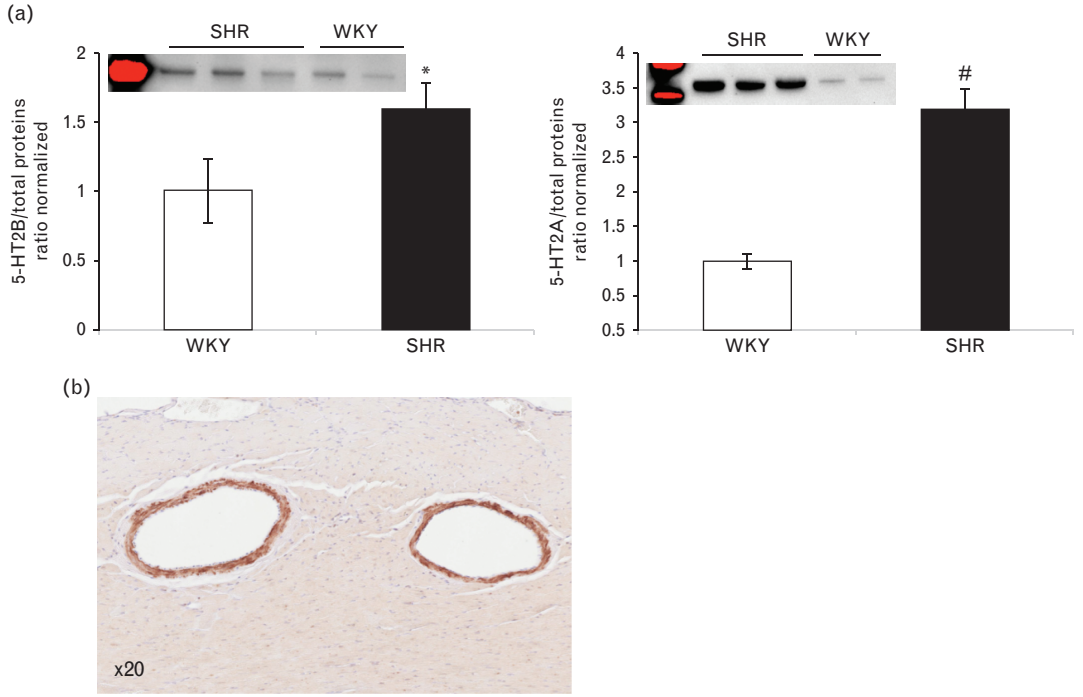

FIGURE 2 Serotonin receptors (5-HT$_{2A}$ and 5-HT$_{2B}$) expression in 51-week-old WKY and SHR hearts. (a) Expression levels of 5-HT$_{2A}$R and 5-HT$_{2B}$R in heart tissues were determined by western blots and normalized by total proteins. Data are means ± SEM. (*) $P < 0.05$ vs. WKYs; (#) $P < 0.01$ vs. WKYs. (b) Localization of the cardiac 5-HT$_{2A}$R mainly in smooth muscle cells of coronary arteries. 5-HT$_{2A}$R, 5-hydroxytryptamine $_{2A}$ receptor; 5-HT$_{2B}$R, 5-hydroxytryptamine $_{2B}$ receptor; SHRs, spontaneously hypertensive rats; WKY, Wistar–Kyoto rats.

Effects of the 5-HT$_{2B}$R antagonist, RS-127445, on cardiac remodeling and cardiovascular hemodynamic

We tested the hypothesis according which the 5-HT$_{2B}$R blockade by a selective antagonist, RS-127445, could affect cardiac hypertrophy, myocardial remodelling, and diastolic dysfunction. As compared with SHR-C rats, RS-127445 mildly, but significantly, reduced SBP (−9 mmHg) without change of HR, cardiac contractility [left ventricular shortening fraction, systolic mitral annulus movement (S_a) measured by Doppler tissue imaging, and invasive dP/dt_{max}], and relaxation (Tables 2 and 3). Left ventricular hypertrophy was also not modified by the antagonist as demonstrated by echocardiography (Table 2), direct cardiac mass measurement, and the QRS maximal amplitude

TABLE 2. Echocardiographic parameters in 43 and 51-week-old spontaneously hypertensive rats

	SHR-C		SHR-N		SHR-RS		SHR-NRS	
	43 WO	51 WO	43 WO	51 WO	43 WO	51 WO	43 WO	51 WO
EDLVD (mm)	7.8 ± 0.5	8.6 ± 0.5	8.1 ± 0.3	8.4 ± 0.5	8.2 ± 0.6	9.3 ± 0.5*	7.7 ± 0.5	8.4 ± 0.3
ESLVD (mm)	3.6 ± 0.5	4.6 ± 0.5	4.4 ± 0.4	4.5 ± 0.7	4.2 ± 0.6	5.4 ± 0.6*	4 ± 0.7	4.7 ± 0.6
SWT (mm)	2 ± 0.08	2.1 ± 0.1	1.8 ± 0.08*	1.68 ± 0.12*	1.9 ± 0.12	1.9 ± 0.1*	1.8 ± 0.05*	1.67 ± 0.06*
PWT (mm)	1.95 ± 0.07	2.03 ± 0.07	1.79 ± 0.07*	1.67 ± 0.06*	1.83 ± 0.1	1.86 ± 0.07*	1.77 ± 0.05*	1.65 ± 0.07*
LVM (mg)	1206 ± 141	1497 ± 163	1110 ± 91*	1079 ± 134*	1189 ± 127	1500 ± 134	1017 ± 130*	1054 ± 90*
LVM index (mg/g)	2.6 ± 0.3	3.25 ± 0.38	2.5 ± 0.22	2.48 ± 0.33*	2.7 ± 0.3	3.38 ± 0.3	2.4 ± 0.26	2.47 ± 0.28*
SF (%)	0.53 ± 0.05	0.46 ± 0.06	0.45 ± 0.04	0.47 ± 0.07	0.48 ± 0.04	0.42 ± 0.05	0.49 ± 0.06	0.44 ± 0.06
Lateral S wave (cm/s)	7.46 ± 1.37	6.54 ± 1.04	6.62 ± 0.78	7.00 ± 1.29	6.89 ± 1.11	6.48 ± 0.74	6.75 ± 0.80	6.00 ± 0.60
E/A	1.5 ± 0.2	1.6 ± 0.4	1.9 ± 0.6*	1.8 ± 0.4	1.9 ± 0.4*	1.7 ± 0.5	1.7 ± 0.46	2.1 ± 0.46*
E wave (cm/s)	131 ± 21	140 ± 20	126 ± 18	123 ± 10	133 ± 11	140 ± 14	127 ± 12	129 ± 11
A wave (cm/s)	91 ± 18	96 ± 30	68 ± 23	69 ± 17	74 ± 23	86 ± 28	77 ± 21	64 ± 20*
IVRT (ms)	24 ± 4	26 ± 3	27 ± 4	27 ± 4	24 ± 4	27 ± 4	25 ± 4	27 ± 3
V_p (cm/s)	25 ± 3	25 ± 2.9	26 ± 4	26 ± 3.5	24 ± 3	25 ± 2.6	23 ± 2	23 ± 3
E_m (cm/s)	4 ± 0.6	4.4 ± 0.4	4.4 ± 0.6	4.3 ± 0.7	4.3 ± 0.7	4.6 ± 0.54	4 ± 0.8	4.1 ± 0.7
E_{pw} (cm/s)	4 ± 0.7	4.1 ± 0.7	4.2 ± 0.4	4.6 ± 0.6	4.1 ± 0.5	4.5 ± 0.71	4.1 ± 0.8	4.3 ± 0.8
E/E_m	33.6 ± 8.5	32 ± 3	29 ± 5	29 ± 3	31 ± 4	31 ± 2.5	33 ± 6.8	32 ± 4.6
ES-LA area (cm^2)	0.38 ± 0.04	0.42 ± 0.03	0.25 ± 0.05	0.42 ± 0.04	0.27 ± 0.05	0.42 ± 0.04	0.23 ± 0.04	0.37 ± 0.03

E, maximal velocity of mitral E wave; E_m, early diastolic velocities at the lateral portion of mitral annulus by Doppler tissue imaging; E_{pw}, early diastolic velocities at the septal portion of mitral annulus by Doppler tissue imaging; EDLVD, end-diastolic left ventricular diameter; ES-LA area, end-systolic left atrium area; ESLVD, end-systolic left ventricular diameter; IVRT, isovolumetric relaxation time; LVM, left ventricular mass; PWT, posterior wall thickness; SF, shortening fraction; SWT, septum wall thickness; V_p, protodiastolic propagation of the E wave (color M-mode); WO, week-old.
*$P < 0.05$ vs. SHR-C at the same age; values are mean ± SD ($n = 10$/group).

TABLE 3. Invasive and noninvasive cardiovascular parameters at the end of the study in spontaneously hypertensive rats

	SHR-C	SHR-N	SHR-RS	SHR-NRS
BW (g)	462 ± 21	443 ± 16	448 ± 15	431 ± 5
SAP (mmHg)	192 ± 11	150 ± 8*	183 ± 12*	148 ± 10*
HR (b.p.m.)	411 ± 60	379 ± 48	395 ± 47	389 ± 43
dP/dt_{max} (mmHg/s)	8584 ± 3281	9756 ± 2243	8646 ± 4290	9221 ± 3954
dP/dt_{min} (mmHg/s)	(−)6906 ± 2375	(−)8141 ± 2264	(−)7000 ± 3070	(−)7960 ± 4280
dP/dt_{min}/LVSP (/s)	49 ± 15	56 ± 13	45 ± 16	50 ± 20
LVEDP (mmHg)	16 ± 6	10 ± 3*	15 ± 4	11 ± 2*
QRS maximal amplitude (mV)	1.1 ± 0.2	0.7 ± 0.3*	0.9 ± 0.2	0.7 ± 0.2*
CM (g)	2.2 ± 0.2	1.95 ± 0.15*	2.2 ± 0.2	1.9 ± 0.1*
CM/BW (g/kg)	4.9 ± 0.5	4.4 ± 0.3	4.9 ± 0.4	4.35 ± 0.5
Plasma BNP (pg/ml)	69 ± 25	37 ± 24*	38 ± 21*	27 ± 18*

BW, body weight; CM, cardiac mass; CM/BW, cardiac mass to body weight ratio; HR, heart rate (assessed by tail-cuff method in conscious 51-week-old rats); LVEDP, left ventricular end-diastolic pressure; SAP, systolic arterial pressure.
dP/dt_{max}, dP/dt_{min}, and dP/dt_{min}/LVSP were obtained by left ventricular catheterization in 52–53-week-old anesthetized rats. Resting QRS maximal amplitude was measured in 52–53-week-old anesthetized rats. Plasma BNP was obtained by ELISA in 52–53-week-old animals. Values are expressed as mean ± SD.
*$P < 0.05$ vs. SHR-C ($n = 10$/group).

(Table 3). Nevertheless, in SHR-RS rats, echocardiography identified that left ventricular end-diastolic and end-systolic diameters were significantly greater than in SHR-C rats, whereas septum wall thickness (SWT) and posterior wall thickness (PWT) were reduced, suggesting that SHR-RS rats further developed eccentric cardiac hypertrophy. Left-atrial dilatation was not affected by RS-127445 and LVEDP was increased similarly as in SHR-C rats. Interestingly, despite the lack of major hemodynamic effect of 5-HT_{2B}R blockade, RS-127445 decreased significantly plasma BNP concentration (−45%) as compared with SHR-C rats (Table 3). RS-127445 did not affect the cardiac 5-HT_{2A}R and 5-HT_{2B}R mRNA overexpression observed in SHR-C rats. Histologically, RS-127445 did not modify perivascular fibrosis, either in large or in small coronary arteries. However, RS-127445 significantly increased interstitial cardiac fibrosis as compared to SHR-C rats (11 ± 5% in SHR-RS vs. 6.7 ± 4% in SHR-C; $P < 0.05$) (Fig. 3a). The increased fibrosis was mainly observed at the subendocardial level (Fig. 4).

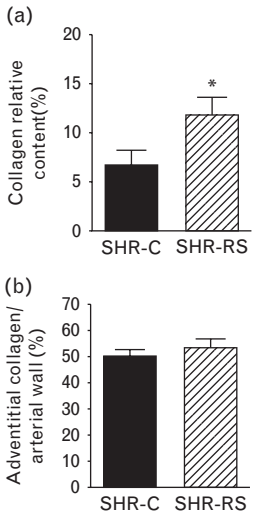

FIGURE 3 Left ventricular fibrosis analyzed by histology. Interstitial (a) and perivascular (b) fibrosis in small coronary vessels were estimated, respectively, by interstitial collagen content and adventitial collagen content, on polarized light using image J software for determining collagen content. The values are mean ± SEM. (*) $P < 0.05$ vs. SHR-C ($n = 10$). SHR, spontaneously hypertensive rat.

Effects of nicardipine on cardiac remodeling and cardiovascular hemodynamic

In 51-week-old SHR-N rats, nicardipine markedly reduced SBP by 42 mmHg and decreased left ventricular hypertrophy as demonstrated by echocardiography, direct cardiac mass measurement, and the decrease of the ECG QRS maximal amplitude (Tables 2 and 3). As compared with SHR-C rats, nicardipine did not modify left ventricular end-diastolic and end-systolic diameters. The left-atrial surface remained unchanged, whereas SWT and PWT were significantly reduced (Table 2). Similarly, the left ventricular systolic function was not modified by the blood pressure reduction as demonstrated by the left ventricular shortening fraction and the systolic mitral annulus movement (S_a) measured by Doppler tissue imaging that remained similar to values obtained in SHR-C rats. The diastolic dysfunction identified in SHR-C rats was not improved by the nicardipine treatment, as attested by Doppler tissue imaging at the mitral annulus, and the IVRT (Table 2). Invasive hemodynamics confirmed echocardiography. Blood pressure reduction did not modify dP/dt_{min}, dP/dt_{max}, and dP/dt_{min}/LVSP. Left ventricular end-diastolic pressure (LVEDP)

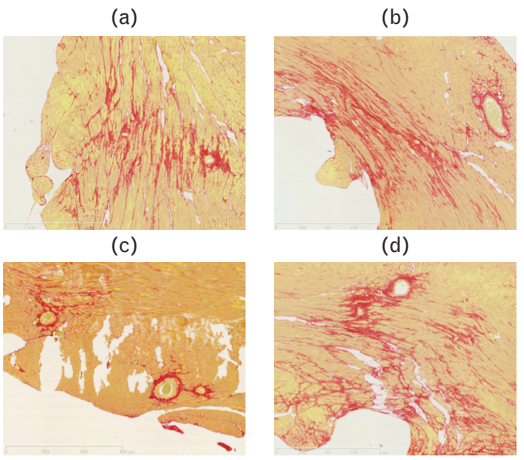

FIGURE 4 Subendocardial fibrosis in vehicle-treated (a) and RS-treated (b) SHRs. Pericoronary fibrosis at the subendocardial level in vehicle-treated (c) and RS-treated (d) SHRs. SHRs, spontaneously hypertensive rats.

decreased significantly. This reduction of LVEDP by nicardipine was associated with a marked decrease in plasma BNP concentration (Table 3). Interestingly, the reduction of blood pressure and left ventricular hypertrophy by nicardipine did not affect the overexpression of 5-HT$_{2B}$R mRNA, but reduced the overexpression of the 5-HT$_{2A}$R mRNA. The mRNA encoding for the serotonin transporter SERT was not significantly affected by this treatment (Fig. 1). In 51-week-old SHR-N rats, nicardipine non-significantly increased interstitial and perivascular collagen deposition (data not shown).

Effects of nicardipine/RS-127445 combination vs. nicardipine alone in cardiac remodeling and cardiovascular hemodynamic

RS-127445 treatment had only minor effects on left ventricular remodeling. We hypothesized that a simultaneous reduction of blood pressure could reveal an effect of 5-HT$_{2B}$R blockade in this model. The association of RS-127445 to nicardipine did not affect the nicardipine blood pressure effect (Table 3). Left ventricular hypertrophy was also reduced in a similar extent as shown by echocardiography, direct cardiac mass measurement, and the decrease of the ECG QRS maximal amplitude (Table 3). The combination of the two drugs did not modify left ventricular systolic function as demonstrated by the left ventricular shortening fraction and the systolic mitral annulus movement (S_a) measured by Doppler tissue imaging. Similarly, left ventricular diastolic dysfunction was not improved as shown by the decrease in DTI early diastolic velocities and IVRT increase in SHR-NRS rats (Table 2). All echocardiographic results were confirmed by invasive hemodynamic evaluation showing no additional effect of RS-127445 on dP/dt_{min}, dP/dt_{max}, and dP/dt_{min}/LVSP. Moreover, LVEDP decreased similarly. Accordingly, BNP plasma level was comparable in the two groups (Table 3). In semiquantitative RT-qPCR, overexpression of either 5-HT$_{2B}$R or 5-HT$_{2A}$R mRNA in SHRs was not modified by nicardipine/RS-127445, although nicardipine alone reduced significantly the 5-HT$_{2A}$R mRNA. SERT mRNA expression was also not different (Fig. 1).

5-HT$_{2B}$ receptor knockout amplifies 5-HT-induced subendocardial myocardial fibrosis in mice

To investigate the mechanisms involved in the subendocardial increase in collagen deposition observed in SHRs chronically treated with RS-127445, we administered 5-HT intraperitoneally during 5 days to wild-type and $Htr_{2B}^{-/-}$ (5-HT$_{2B}$R knockout) mice. In wild-type animals, 5-HT induced focal areas of cell proliferation in myocardium as attested by Ki67 labeling (Fig. 5), in which numerous vimentin-positive cells were observed. These foci were localized at the subendocardial and mid-wall level. The 5-HT-induced myocardial fibrosis was increased in $Htr_{2B}^{-/-}$ animals as attested by the increased Ki67 and vimentin labeling. In contrast, 5-HT-induced cell proliferation (Ki67) was completely blocked in both $Htr_{2A}^{-/-}$ and $Htr_{2A/2B}^{-/-}$ mice (Fig. 5). As a consequence, fibrosis was not observed (data not shown).

5-HT$_{2B}$ receptor is involved in arterial vasodilatation

To investigate a putative contribution of 5-HT$_{2B}$Rs in the regulation of arterial vasomotion, we first analyzed coronary artery resistances in isolated hearts obtained from wild-type and $Htr_{2B}^{-/-}$ males. Baseline coronary resistance was increased by 11.4% in $Htr_{2B}^{-/-}$ animals compared to the wild type. This difference was maintained during isoproterenol infusion without reaching statistical significance due to variability in transgenic mice (Fig. 6a). To deeply explore the contribution of 5-HT$_{2B}$R during vascular 5-HT$_2$R stimulation, we studied the effects of the 5-HT$_2$R agonist, α-methyl-5-HT (AMS), on aortic rings obtained from wild-type and $Htr_{2B}^{-/-}$ mice. This compound induced a concentration-dependent aortic constriction in wild-type animals, indicating that the resulting effect of global vascular 5-HT$_2$R stimulation is vasoconstriction. Nevertheless, the genetic ablation of Htr_{2B} significantly increased by 58% the effect of AMS, showing that this agonist has a dual effect on blood vessels, the vasodilatation component being mediated by the 5-HT$_{2B}$R subtype (Fig. 6b). Then, we hypothesized that this role of the 5-HT$_{2B}$R could involve endothelial nitric oxide synthase and the guanylate cyclase pathway. In $Htr_{2B}^{-/-}$ mice, we identified an important reduction of cGMP aortic content compared to wild type and, on the contrary, an amplified response to the nitric oxide donor, S-N-acetylpenicillamine (Fig. 6c).

DISCUSSION

The present study shows that the selective 5-HT$_{2B}$R antagonist, RS-127445, induces left ventricular dilatation and promotes subendocardial fibrosis during the natural course of hypertensive cardiomyopathy in SHRs, a model of DD-PEF with 5-HT$_{2A/2B}$R overexpression. Moreover, this compound fails to improve diastolic dysfunction even if blood pressure is reduced by nicardipine. A subendocardial left ventricular fibrosis induced by 5-HT in wild-type mice is amplified in $Htr_{2B}^{-/-}$ animals, but prevented in $Htr_{2A}^{-/-}$ and $Htr_{2A/2B}^{-/-}$. Finally, in-vitro experiments conducted in aortic rings demonstrate the contribution of endothelial 5-HT$_{2B}$ receptor to arterial vasodilatation.

The naturally occurring cardiac disease of SHRs shows many similarities to human essential hypertension. Diastolic ventricular dysfunction occurs quickly after a few weeks of high blood pressure, whereas cardiac systolic function remains stable for a long period [12,18,19]. Upon aging, SHRs progressively display all typical features of DD-PEF: hypertension, cardiac hypertrophy, diastolic dysfunction, apparently preserved contractility, and collagen deposit.

To investigate a possible role of 5-HT in cardiac remodeling associated with diastolic dysfunction, we choose the selective 5-HT$_{2B}$R antagonist, RS-127445, for different reasons: this compound is highly selective with a high affinity ($pKi = 9.5 \pm 0.1$) and high potency ($pIC_{50} = 10.4 \pm 0.1$) towards 5-HT$_{2B}$Rs [13]; pharmacokinetic data are available for this compound in rats. In this species, the absolute bioavailability is quite poor (14%) by oral administration, but markedly better following intraperitoneal injection (62%) [13]; in previous studies, this compound showed a good

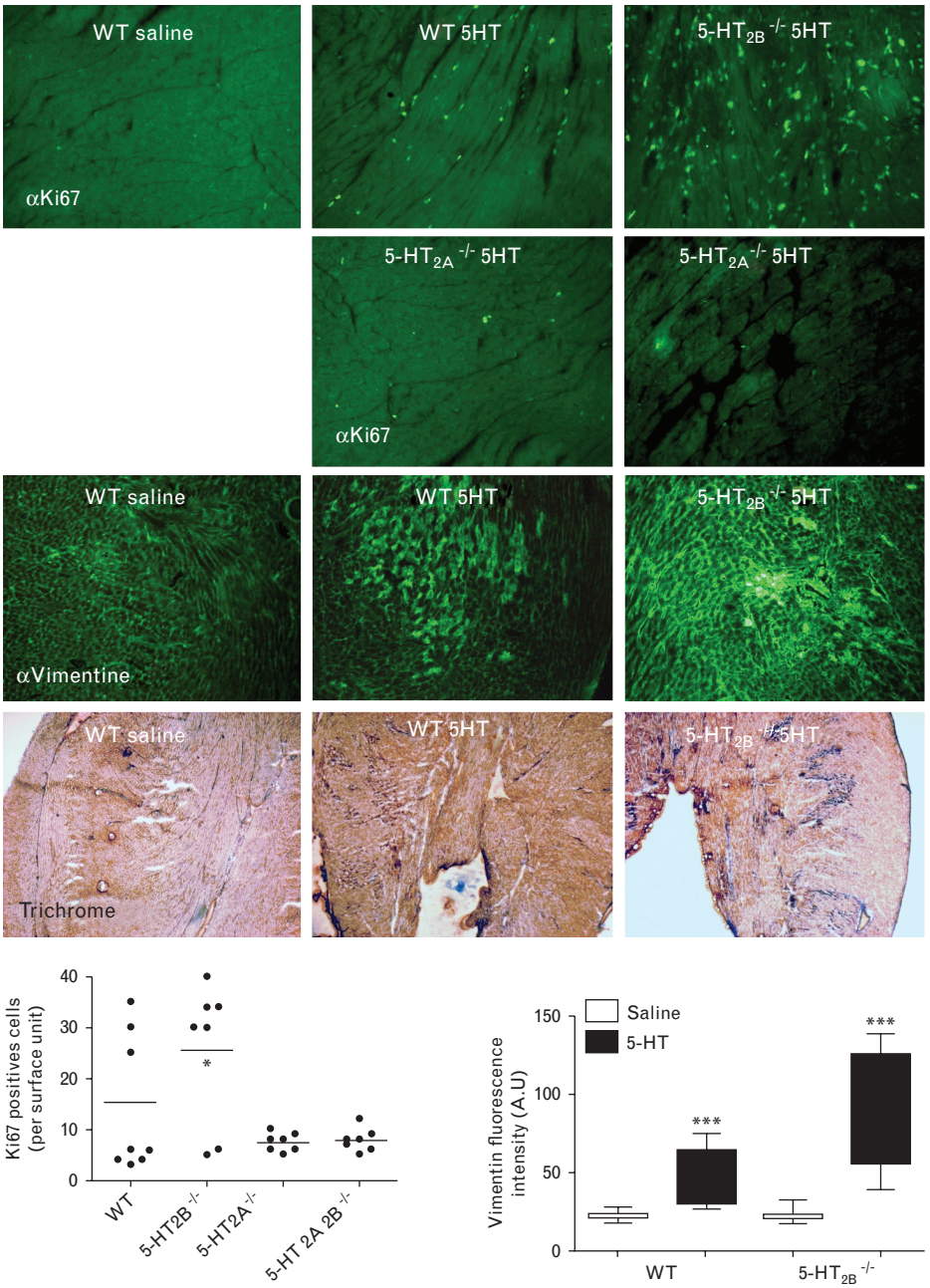

FIGURE 5 Wild-type and 5-$HT_{2B}^{-/-}$ male mice ($n = 8$/group) were treated by 5-HT i.p. injection (or saline as control) during 5 days. Both genotype responded to 5-HT by increasing Ki67-positive cells with a stronger effect seen in 5-$HT_{2B}R^{-/-}$ (upper panel). Using anti-vimentin antibody and trichrome staining, we confirmed the observation that Ki67-positive cells are in interstitial cells. Quantification of Ki67 and vimentin staining are shown in the lower panel. Unpaired *t* test and one-way ANOVA with Bonferoni post-hoc test were used for Ki67 and vimentin quantification, respectively.(*) $P < 0.05$; (***) $P < 0.001$ ($n = 8$). 5-HT_{2B}R, 5-hydroxytryptamine $_{2B}$ receptor; ANOVA, analysis of variance.

efficacy at the 1 mg/kg per day dose in rats and mice [13,20]. Two injections/day were selected in regard to the plasma half-life of the drug in rats (≈6 h) [13], and we treated the animals by two intraperitoneal injections of 500 μg/kg each during 14 weeks. In these conditions, RS-127445 did not reduce cardiac hypertrophy despite the 5-HT_{2B}R mRNA overexpression in 51-week-old SHRs, as previously observed in other situations of left ventriular dysfunction [11,21]. This result contrasts with previous published papers showing that 5-HT_{2B}R blockade prevents cardiac hypertrophy in mouse models of isoproterenol and angiotensin II infusions, as well as in aortic-banded rats [11,21]. However, the serotonergic system seems not affected in SHRs since no difference in 24-h urinary 5-HIAA excretion was noticed in SHRs compared to WKY rats, attesting an apparent normal 5-HT turnover in these hypertensive animals. Moreover, RS-127445 is not a 5-HT_{2B}R inverse agonist as compared to other 5-HT_{2B}R ligands, such as SB215505 or SB206553 [13]. These data could explain the RS-127445 inability to affect the 5-HT_{2B}R pathway in the absence of 5-HT. Nevertheless, as shown by the 24-h urinary epinephrine excretion, the sympathetic nervous system is stimulated in these animals, and an interaction between β-adrenoceptors and the 5-HT_{2B}R was previously demonstrated for cardiac hypertrophy [9,21].

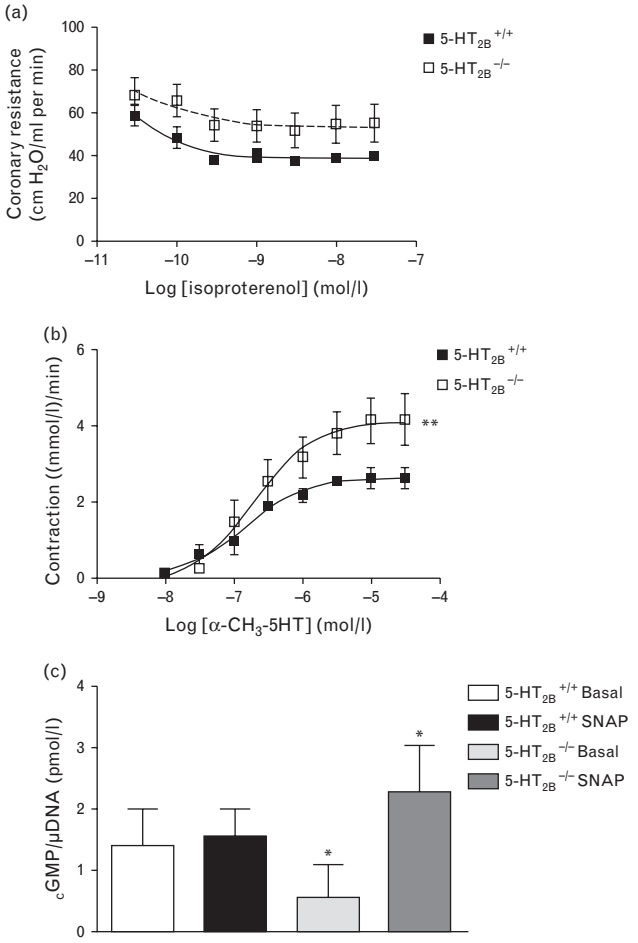

FIGURE 6 Involvement of the 5-HT$_{2B}$R in arterial vasodilation. (a) Concentration–response effect of isoproterenol on coronary artery resistances of isolated hearts obtained from male wild-type ($n=7$) and *Htr*$_{2B}^{-/-}$ mice ($n=6$). A non-significant difference of 11% was observed at baseline that was maintained when increasing isoproterenol concentrations. (b) Concentration–response effect of α-methyl-5-HT (AMS) on the contraction of aortic isolated rings obtained from wild-type and *Htr*$_{2B}^{-/-}$ male mice ($n=7$/genotype). The absence of the 5-HT$_{2B}$R amplified the AMS constriction by 58%. (c) cGMP content in aorta at baseline and after S-N-acetylpenicillamine (SNAP) application showing a reduced baseline concentration in *Htr*$_{2B}^{-/-}$ mice, but an amplified response to SNAP. Values are expressed as mean ± SEM. (**) $P<0.01$; (*) $P<0.05$: wild-type vs. *Htr*$_{2B}^{-/-}$ mice. 5-HT$_{2A}$R, 5-hydroxytryptamine $_{2A}$ receptor; 5-HT$_{2B}$R, 5-hydroxytryptamine $_{2B}$ receptor.

But, here again, such a mechanism may not be strong enough to obtain an RS-127445 effect in SHRs.

One explanation to this lack of efficacy is that cardiac hypertrophy is load-dependent in SHRs, a contribution of neurohumoral pathways being only marginally involved. To test this hypothesis, we used the calcium channel blocker, nicardipine. This compound markedly reduces cardiac hypertrophy in parallel with blood pressure reduction. An additional antihypertrophic effect of RS-127445 when combined to nicardipine was not obtained. These data argue in favor of the high load-dependence of cardiac hypertrophy in this model. On the contrary, in cardiac hypertrophy due to aortic banding in rats, Liang *et al.* [11] found a prevention of the left ventricular hypertrophy by the 5-HT$_{2B}$R antagonist, SB215505. This effect was associated with a reduction of plasma BNP. In our study, plasma BNP was markedly diminished by RS-127445 despite a small blood pressure decrease and no cardiac hypertrophy reduction, ruling out any contribution of a decreased cardiac wall stress in this effect. Therefore, the 5-HT$_{2B}$R could be involved in an intracellular mechanism activating BNP expression independently of hypertrophy and loading conditions. It was previously suggested that this cellular event could involve the nuclear factor (NF)-kappaB [11]. In the RS-127445 group, we observed an increase in left ventricular end-diastolic diameter, indicating an eccentric hypertrophy and perhaps the beginning of left ventricular dilatation. This phenomenon occurs in the absence of systolic failure, but we identified an increase in collagen deposit similar to scarring plaques at the subendocardial level. These profibrotic events induced by 5-HT$_{2B}$R blockade are contrasting with our previous mice studies in which blocking this receptor in non-cardiomyocyte cells was associated with a marked reduction of oxidative stress and inflammatory cytokine production [9,10].

In order to rule out species differences and to analyze the contribution of this receptor in myocardial fibrosis, we investigated the effects of a systemic daily injection of a high dose of 5-HT over 5 days on left ventricular fibrosis in mice. In wild-type mice, 5-HT-induced subendocardial and mid-wall myocardial scars similar to those observed in SHRs. In these healing processes, cell proliferation is observed and numerous cells are vimentin-positive, that is, fibroblasts and/or myofibroblasts. Interestingly, the genetic ablation of 5-HT$_{2B}$Rs in *Htr*$_{2B}^{-/-}$ mice amplified this phenomenon, indicating a protective, anti-fibrotic role of the 5-HT$_{2B}$R subtype. In fact, blockade of the 5-HT$_{2B}$R could reveal the fibrogenic contribution of other serotonergic receptors. In the whole left ventricular myocardium, we observed a marked overexpression of the 5-HT$_{2A}$R both at the mRNA and protein level. In rats, this receptor is expressed in various cell types, including ventricular fibroblasts. 5-HT, by stimulating the 5-HT$_{2A}$R, promotes the proliferation, differentiation into myofibroblasts, migration, and TGF-β1 secretion by these cells [22]. To determine the contribution of 5-HT$_{2A}$Rs, mice carrying a knockout for this receptor or for both 5-HT$_{2A}$ and 5-HT$_{2B}$ subtypes were subjected to 5 days of 5-HT injection. These animals were fully protected from 5-HT-induced fibroblast proliferation and myocardial fibrosis, suggesting a 5-HT$_{2A}$R/5-HT$_{2B}$R balance on fibroblast/myofibroblast activity into the myocardium. At the opposite to 5-HT$_{2B}$Rs, 5-HT$_{2A}$Rs overexpression could contribute to the maintenance of myocardial contractility but with fibrosis as a deleterious counterpart. Some authors described an expression mainly at the cardiomyocyte level, and the contribution of its activation to contractility increases in parallel with the extent of hypertrophy [23]. In our study, we show an important expression in the arterial wall that is probably dependent on the afterload level because it is reduced by nicardipine. We cannot rule out an effect that would also take place at the cardiomyocyte level.

Concerning the 5-HT$_{2B}$R, we have observed an overexpression in the LV of the SHRs. At the mRNA level, this overexpression is higher than previously described [24]. It is not sensitive to blood pressure-lowering and cardiac hypertrophy reduction by nicardipine and, therefore, appears as load-independent. The relevance of this overexpression to

the pathophysiology of DD-PEF is unknown. We have observed a similar pattern in humans showing a left ventricular systolic failure [21], and Brattelid *et al.* [24] identified such an overexpression only in failing rats. This result could be the hallmark of a progressive evolution towards heart failure of old SHRs and/or be associated with hypertensive cardiomyopathy. At the arterial wall level, a similar overexpression was described by Watts and Fink [25] in deoxycorticosterone (DOCA) salt-hypertensive rats. In their experiments, DOCA salt identified two groups of responders. Some of the animals became severely hypertensive (DOCA-S) and responded to the 5-HT_{2B}R antagonist LY272015 by a reduction of the blood pressure. Another group developed a moderate hypertension (DOCA-M) and, at the opposite, displayed a mild pressure response to the same compound [25]. When the endothelium was removed, mesenteric arteries from DOCA salt rats showed a concentration-dependent contraction when exposed to the 5-HT_{2B} R-selective agonist BW723C86. We can suspect a dual role of the 5-HT_{2B}R on vasomotor control: vasoconstriction mediated by receptors expressed at the smooth muscle cell level together with 5-HT_{2A} receptors and vasodilatation involving endothelial nitric oxide synthase at the endothelium level. In the present study, RS-127445 reduced systemic blood pressure by 9 mmHg, confirming, in another model and with another antagonist, the results obtained in DOCA-S rats with LY272015.

To move further into this hypothesis, we conducted ex-vivo experiments in isolated hearts and aortic preparations obtained from wild-type and $Htr_{2B}^{-/-}$ mice. Basal coronary arterial resistance showed a tendency to an increase (+11%) that was maintained when the cardiac work was increased by the mixed β_1/β_2 adrenergic agonist, isoproterenol. The variability of the preparation in knockout mice was probably due to their cardiomyocyte phenotype as previously described and limited our investigation. Therefore, we analyzed the response of aortic rings exposed to the 5-HT_2R agonist, AMS. This drug activates both 5-HT_{2A} and 5-HT_{2B}Rs and induces a concentration-dependent vasoconstriction in wild-type animals, indicating that the activation of these receptors located in arterial smooth muscle cells leads mainly to vasoconstriction. Interestingly, the genetic ablation of the 5-HT_{2B}R subtype markedly amplified the response. This result emphasizes that this receptor subtype is involved in vasodilatation following serotonergic stimulation. In fact, this receptor is expressed by endothelial cells, and is coupled to endothelial nitric oxide synthase/cGMP pathway [26]. The absence of the receptor in $Htr_{2B}^{-/-}$ mice reduces basal cGMP vascular synthesis, attesting a reduced nitric oxide production and/or the repression of guanylate cyclase. The last was not confirmed because the response to the nitric oxide donor, N-S-acetylpenicillamine, was amplified, suggesting a putative compensation of the reduced nitric oxide synthesis in these animals. Taking together, these data show that the endothelial 5-HT_{2B}R contributes to arterial vasodilatation. Its absence or blockade could, in certain circumstances, participate to vasospasms and ischemic events. Nevertheless, these mice data were obtained in the aorta and will have to be confirmed in coronary arteries.

The main objective of this study was to evaluate the effect of RS-127445 on the diastolic function. One-year-old SHRs demonstrate troubles of the early diastole as attested by changes in IVRT, V_p, E_m, and E_{pw}. These alterations were affected neither by blood pressure reduction nor by 5-HT_{2B}R antagonism or the combination of both. Change in the first diastolic phase is usually considered as an abnormality of the diastolic calcium capture into the sarcoplasmic reticulum. We did not observe any change of the sarcoplasmic reticulum Ca^{2+} ATPase (SERCA-2a) expression at the mRNA level in SHRs (data not shown), but some studies have shown that cardiac dysfunction could be associated with a reduction of the SERCA-2a protein stability rather than reduced transcription. Such a trouble was not sensitive to 5-HT_{2B}R blockade and not improved by blood pressure lowering in SHRs.

The present study is the first to investigate the role of the 5-HT_{2B}R in a model of DD-PEF. It reveals that this receptor is overexpressed in the disease, but could be protective from myocardial fibrosis. The 5-HT_{2B}R antagonism reveals the activation of other overexpressed receptors (such as the 5-HT_{2A}R) that could explain increased fibrosis when the 5-HT_{2B}R subtype is blocked. The marked overexpression of the two main subtypes of 5-HT_2Rs in the heart supports the contribution of the serotonergic system in DD-PEF with different but opposite contribution of 5-HT_{2A}Rs and 5-HT_{2B}Rs.

ACKNOWLEDGEMENTS

Claudia de Tapia (Laboratoire de Neurobiologie et Pharmacologie Cardiovasculaire), Patrice Goetz-Reiner, and Isabelle Tilly (Mouse Clinical Institute) are thanked for their technical assistance.

The present study was supported by the Centre National de la Recherche Scientifique, the Institut National de la Santé et de la Recherche Médicale, the Paris Université Pierre et Marie Curie, the University of Strasbourg, the Centre Hospitalier et Universitaire de Strasbourg, and by grants from the Fondation de France, the French Ministry of Research, Agence Nationale pour la Recherche (ANR-12-BSV1-0015-01), S. Doly was supported by a Lefoulon-Lalande fellowship. L. Maroteaux's team is part of the École des Neurosciences de Paris Ile-de-France network and of the Bio-PsyLabex.

Conflicts of interest

There are no conflicts of interest.

REFERENCES

1. Cleland JG, Swedberg K, Follath F, Komajda M, Cohen-Solal A, Aguilar JC, *et al.* The EuroHeart Failure survey programme: a survey on the quality of care among patients with heart failure in Europe. Part 1: patient characteristics and diagnosis. *Eur Heart J* 2003; 24:442–463.
2. Lenzen MJ, Scholte op Reimer WJ, Boersma E, Vantrimpont PJ, Follath F, Swedberg K, *et al.* Differences between patients with a preserved and a depressed left ventricular function: a report from the EuroHeart Failure Survey. *Eur Heart J* 2004; 25:1214–1220.
3. Massie BM, Carson PE, McMurray JJ, Komajda M, McKelvie R, Zile MR, *et al.* Irbesartan in patients with heart failure and preserved ejection fraction. *N Engl J Med* 2008; 359:2456–2467.
4. Yusuf S, Pfeffer MA, Swedberg K, Granger CB, Held P, McMurray JJ, *et al.* Effects of candesartan in patients with chronic heart failure and

preserved left-ventricular ejection fraction: the CHARM-Preserved Trial. *Lancet* 2003; 362:777–781.
5. Akhter SA, Luttrell LM, Rockman HA, Iaccarino G, Lefkowitz RJ, Koch WJ. Targeting the receptor-Gq interface to inhibit in vivo pressure overload myocardial hypertrophy. *Science* 1998; 280:574–577.
6. Colombo F, Noel J, Mayers P, Mercier I, Calderone A. beta-Adrenergic stimulation of rat cardiac fibroblasts promotes protein synthesis via the activation of phosphatidylinositol 3-kinase. *J Mol Cell Cardiol* 2001; 33:1091–1106.
7. Nebigil CG, Hickel P, Messaddeq N, Vonesch JL, Douchet MP, Monassier L, *et al.* Ablation of serotonin 5-HT(2B) receptors in mice leads to abnormal cardiac structure and function. *Circulation* 2001; 103:2973–2979.
8. Nebigil CG, Jaffre F, Messaddeq N, Hickel P, Monassier L, Launay JM, *et al.* Overexpression of the serotonin 5-HT2B receptor in heart leads to abnormal mitochondrial function and cardiac hypertrophy. *Circulation* 2003; 107:3223–3229.
9. Jaffre F, Callebert J, Sarre A, Etienne N, Nebigil CG, Launay JM, *et al.* Involvement of the serotonin 5-HT2B receptor in cardiac hypertrophy linked to sympathetic stimulation: control of interleukin-6, interleukin-1beta, and tumor necrosis factor-alpha cytokine production by ventricular fibroblasts. *Circulation* 2004; 110:969–974.
10. Monassier L, Laplante MA, Jaffre F, Bousquet P, Maroteaux L, de Champlain J. Serotonin 5-HT(2B) receptor blockade prevents reactive oxygen species-induced cardiac hypertrophy in mice. *Hypertension* 2008; 52:301–307.
11. Liang YJ, Lai LP, Wang BW, Juang SJ, Chang CM, Leu JG, *et al.* Mechanical stress enhances serotonin 2B receptor modulating brain natriuretic peptide through nuclear factor-kappaB in cardiomyocytes. *Cardiovasc Res* 2006; 72:303–312.
12. Marzak H, Ayme-Dietrich E, Lawson R, Mokni W, Combe R, Becker J, *et al.* Old spontaneously hypertensive rats gather together typical features of human chronic left-ventricular dysfunction with preserved ejection fraction. *J Hypertens* 2014; 32:1307–1316.
13. Bonhaus DW, Flippin LA, Greenhouse RJ, Jaime S, Rocha C, Dawson M, *et al.* RS-127445: a selective, high affinity, orally bioavailable 5-HT2B receptor antagonist. *Br J Pharmacol* 1999; 127:1075–1082.
14. Gonzàlez-Maeso J, Yuen T, Ebersole BJ, Wurmbach E, Lira A, Zhou M, *et al.* Transcriptome fingerprints distinguish hallucinogenic and non-hallucinogenic 5-hydroxytryptamine 2A receptor agonist effects in mouse somatosensory cortex. *J Neurosci* 2003; 23:8836–8843.
15. Nebigil CG, Choi D-S, Dierich A, *et al.* Serotonin 2B receptor is required for heart development. *Proc Natl Acad Sci U S A* 2000; 97:9508–9513.
16. Matz RL, de Sotomayor MA, Schott C, Stoclet JC, Andriantsitohaina R. Vascular bed heterogeneity in age-related endothelial dysfunction with respect to NO and eicosanoids. *Br J Pharmacol* 2000; 131:303–311.
17. Martínez MC, Muller B, Stoclet JC, Andriantsitohaina R. Alteration by lipopolysaccharide of the relationship between intracellular calcium levels and contraction in rat mesenteric artery. *Br J Pharmacol* 1996; 118:1218–1222.
18. Cingolani OH, Yang XP, Cavasin MA, Carretero OA. Increased systolic performance with diastolic dysfunction in adult spontaneously hypertensive rats. *Hypertension* 2003; 41:249–254.
19. Dupont S, Maizel J, Mentaverri R, Chillon JM, Six I, Giummelly P, *et al.* The onset of left ventricular diastolic dysfunction in SHR rats is not related to hypertrophy or hypertension. *Am J Physiol Heart Circ Physiol* 2012; 302:H1524–H1532.
20. Launay JM, Herve P, Peoc'h K, Tournois C, Callebert J, Nebigil CG, *et al.* Function of the serotonin 5-hydroxytryptamine 2B receptor in pulmonary hypertension. *Nature Med* 2002; 8:1129–1135.
21. Jaffre F, Bonnin P, Callebert J, Debbabi H, Setola V, Doly S, *et al.* Serotonin and angiotensin receptors in cardiac fibroblasts coregulate adrenergic-dependent cardiac hypertrophy. *Circ Res* 2009; 104:113–123.
22. Yabanoglu S, Akkiki M, Seguelas MH, Mialet-Perez J, Parini A, Pizzinat N. Platelet derived serotonin drives the activation of rat cardiac fibroblasts by 5-HT2A receptors. *J Mol Cell Cardiol* 2009; 46:518–525.
23. Brattelid T, Qvigstad E, Birkeland JA, Swift F, Bekkevold SV, Krobert KA, *et al.* Serotonin responsiveness through 5-HT2A and 5-HT4 receptors is differentially regulated in hypertrophic and failing rat cardiac ventricle. *J Mol Cell Cardiol* 2007; 43:767–779.
24. Brattelid T, Tveit K, Birkeland JA, Sjaastad I, Qvigstad E, Krobert KA, *et al.* Expression of mRNA encoding G protein-coupled receptors involved in congestive heart failure: a quantitative RT-PCR study and the question of normalisation. *Basic Res Cardiol* 2007; 102:198–208.
25. Watts SW, Fink GD. 5-HT2B-receptor antagonist LY-272015 is antihypertensive in DOCA-salt-hypertensive rats. *Am J Physiol* 1999; 276 (3 Pt 2):H944–H952.
26. Manivet P, Mouillet-Richard S, Callebert J, Nebigil CG, Maroteaux L, Hosoda S, *et al.* PDZ-dependent activation of nitric-oxide synthases by the serotonin 2B receptor. *J Biol Chem* 2000; 275:9324–9331.

Reviewers' Summary Evaluations

Referee 1

In testing the hypothesis that blockade of the serotonin (5-HT)2B receptor will protect the heart of spontaneously hypertensive rats from diastolic dysfunction the authors unexpectedly found that blockade of 5-HT2$_{BR}$ by RS-127445 led to an increase in fibrosis and left ventricular dilatation. The study points to the contrasting roles of the 5-HT2R sub-types in cardiac remodeling associated with preserved ejection ratio heart failure. The results also highlight that, whilst we no longer consider heart failure to be a single diagnosis, the complex array of underlying causes and disease presentation needs to be reflected in our animal models and our interpretation of the data from these models.

Referee 2

In this study, Ayme-Dietrich *et al.* investigated the effects of chronic inhibition of serotonin (5-HT)2B receptors in reducing left ventricular remodeling and dysfunction in old SHR. Surprisingly, no beneficial effects were observed with the specific 5-HT2$_{BR}$ inhibitor RS-127445, and even more fibrosis was induced, mostly subendocardially. A complementary study in mice knockout for 5-HT2$_{BR}$, 5-HT2$_{AR}$, or both suggests opposing effects of the two main 5-HT2$_{R}$ on fibrosis and arterial vasodilation. Further studies are needed to reveal whether the 5-HT2$_{BR}$/5-HT2$_{AR}$ dysbalance affects primarily fibroblast or induces ischemia since in vitro experiments on aortic rings will have to be confirmed in coronary arteries.